Title
Conceptual design of a fast-ion D-alpha diagnostic on experimental advanced superconducting tokamak.

Journal
The Review of scientific instruments, 85(11)

ISSN
0034-6748

Authors
Huang, J
Heidbrink, WW
Wan, B
et al.

Publication Date
2014-11-01

DOI
10.1063/1.4887820

Conceptual design of a fast-ion D-alpha diagnostic on experimental advanced superconducting tokamak[a)]

J. Huang,[1,b)] W. W. Heidbrink,[2] B. Wan,[1] M. G. von Hellermann,[3] Y. Zhu,[2] W. Gao,[4] C. Wu,[4] Y. Li,[4] J. Fu,[4] B. Lyu,[4] Y. Yu,[4] Y. Shi,[4,5] M. Ye,[4] L. Hu,[1] and C. Hu[1]
[1]*Institute of Plasma Physics, Chinese Academy of Sciences, P.O. 1126, 230031 Hefei, Anhui, China*
[2]*Department of Physics and Astronomy, University of California, Irvine, California 92697, USA*
[3]*FOM Institute DIFFER, P.O. BOX 1207, Nieuwegein 3430 BE, The Netherlands*
[4]*School of Nuclear Science and Technology, University of Science and Technology of China, Hefei, Anhui 230026, China*
[5]*WCI for Fusion Theory, National Fusion Research Institute, 52 Eoeun-Dong, Yusung-Gu, Daejeon 305-333, South Korea*

(Presented 4 June 2014; received 28 May 2014; accepted 22 June 2014; published online 17 July 2014)

To investigate the fast ion behavior, a fast ion D-alpha (FIDA) diagnostic system has been planned and is presently under development on Experimental Advanced Superconducting Tokamak. The greatest challenges for the design of a FIDA diagnostic are its extremely low intensity levels, which are usually significantly below the continuum radiation level and several orders of magnitude below the bulk-ion thermal charge-exchange feature. Moreover, an overlaying Motional Stark Effect (MSE) feature in exactly the same wavelength range can interfere. The simulation of spectra code is used here to guide the design and evaluate the diagnostic performance. The details for the parameters of design and hardware are presented. © *2014 AIP Publishing LLC*. [http://dx.doi.org/10.1063/1.4887820]

I. INTRODUCTION

In present day fusion devices, with the development of high power external heating systems, such as neutral beam injection and wave heating at radio frequencies, the study of the fast-ion behavior becomes more important to understand their confinement. One powerful diagnostic method is the fast-ion D-alpha (FIDA) technique, which is based on charge-exchange between injected neutral beam particles and the high energetic deuterium ions, similar as the measurements of energetic helium ions reported on Joint European Torus (JET) in 1993.[1] Since it was first successfully exploited in Doublet-III-D (DIII-D),[2] now it has been applied to several tokamaks (National Spherical Torus Experiment (NSTX);[3] Tokamak EXperiment for Technology Oriented Research (TEXTOR);[4] Axially Symmetric Divertor EXperiment Upgrade (ASDEX-U)[5]). Similar experiments based on Fast Ion Charge eXchange Spectroscopy (FICXS) have been applied on Large Helical Device (LHD).[6]

To investigate the fast ion behavior on EAST (Experimental Advanced Superconducting Tokamak), FIDA diagnostic system has been planned and is presently under development. For the EAST active beam induced diagnostic design, the **S**imulation **O**f **S**pectra code (SOS)[7] has been applied for the diagnostic performance studies. An essential input is a comprehensive modelling effort based on charge-exchange (CX) analysis packages developed and validated during the past two decades on fusion devices such as JET, TEXTOR, ASDEX-U, and Tore Supra.

The paper is organized as follows. The fast ion spectra modelling code will be introduced in Sec. II. The measurement evaluation and prediction will be described in Sec. III. Planned layout and instrument performance will be presented in Sec. IV.

II. MODELLING OF FAST ION SPECTRA IN SIMULATION OF SPECTRA CODE

SOS code addresses three different types of active beam induced spectra plus associated background spectra comprising: (1) thermal fully stripped impurity ion CX spectra, (2) MSE and bulk-ion CX spectra, (3) fast ion CX spectroscopy, including slowing-down fusion alphas and slowing-down beam ions.

The resulting spectrum is a convolution of the effective CX emission rate $Q_{cx}(v_r)$ and the slowing-down velocity distribution function g_{slow},[1] which is for the fast beam ion in this case:

$$f_{obs}(v_z) = \int_0^\infty v' 2dv' \int_0^\pi d\theta' \sin\theta' \int_0^{2\pi} d\varphi' \; g_{slow}(v', \theta', \varphi') Q_{CX}(v_r) \delta(v_z - v' \cos\theta'), \quad (1)$$

where v_r is the collision velocity between the fast ion and beam particle, v' and v_b. The angles in observation frame are θ and φ. The direction of observation is in positive z-direction, and θ is the angle between viewing line and v'. As the slowing-down function, we use the anisotropic function from the analytical solution of the neutral injection Fokker-Planck equation. δ-function refers to particles moving either away or toward the observer.

For the calculation of the observed spectral intensity, we need to calculate the fast ion density which depends primarily

[a)]Contributed paper, published as part of the Proceedings of the 20th Topical Conference on High-Temperature Plasma Diagnostics, Atlanta, Georgia, USA, June 2014.
[b)]Electronic mail: juan.huang@ipp.ac.cn

on the fast ion source rate, the slowing-down time and the local probe beam density. In the case of steady state condition ($t \gg \tau_s$, where τ_s is slowing-down time, with the EAST case discussed in Sec. III, τ_s with about 0.2 s) and a positive ion beam source with three energy species, the local fast ion density and fast-ion CX signal are obtained, respectively,

$$n_{fast-ion}(\rho) = \frac{1}{3}\tau_s(\rho)\sum_{k=1}^{k=3} S_k(\rho)\cdot \ln\left[1+\left(\frac{v_{b,k}}{v_c(\rho)}\right)^3\right], \quad (2)$$

$$I^{cx}_{fast-ion}(\lambda,\rho) = \frac{1}{4\pi}\sum_{k=1}^{k=3}\sum_{i=1}^{3} n_k^{probe-beam}(\rho) \cdot n_i^{fast-ion}(\rho)\cdot f^{fast-ion}_{obs,i}(\lambda,\rho), \quad (3)$$

where v_b, v_c are the injection and critical velocity, respectively. $S(\rho)$ is the neutral beam source rate, derived from the local beam attenuation factor ζ along the entire beam trajectory, as calculated from local beam stopping data $\sigma_{stop,z}$, local electron density n_e, and impurity ion $c_z = n_z/n_e$:

$$S = \frac{P_{beam}}{e\cdot E_{beam}}\cdot\frac{\partial\zeta}{\partial V}, \quad (4)$$

$$\zeta = \exp\left[-\int_{beam-path} ds\cdot n_e\cdot\sum_z c_z\cdot\sigma_{stop,z}\right], \quad (5)$$

where P_{beam} is the power of beam, and E_{beam} is the energy of beam.

III. MEASUREMENT PREDICTIONS

A. EAST neutral beam and source rate evaluation

Figure 1 shows the two proposed neutral beam injector systems on the A port and F port of the EAST tokamak, respectively. For the coming campaign in 2014, the available injector will be on the A port, including two beam sources. The more tangential beam will be viewed by FIDA technique, which can produce 2–4 MW beam power with 50–80 keV beam energy, with the power fraction 80%:14%:6% for each full, half, and third energy component.

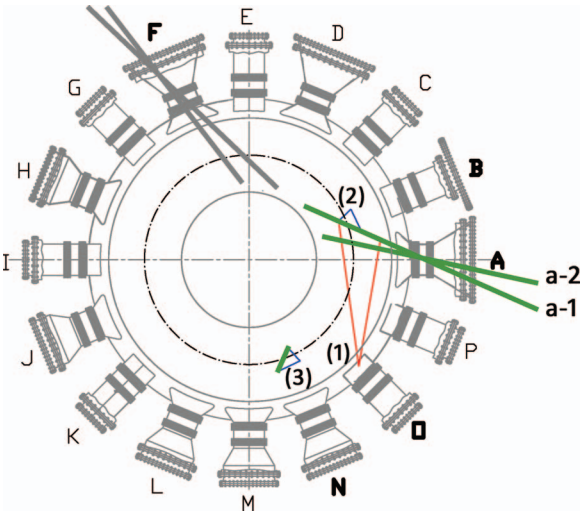

FIG. 1. Top view for the EAST tokamak with two proposed neutral beam injector systems on the available A-port, including two beam sources (a-1, a-2), and the future F-port. The more tangential beam (a-1) will be viewed by FIDA with planned (1) tangential active view from O-port, (2) vertical active view from B-port, and (3) vertical passive view from N-port.

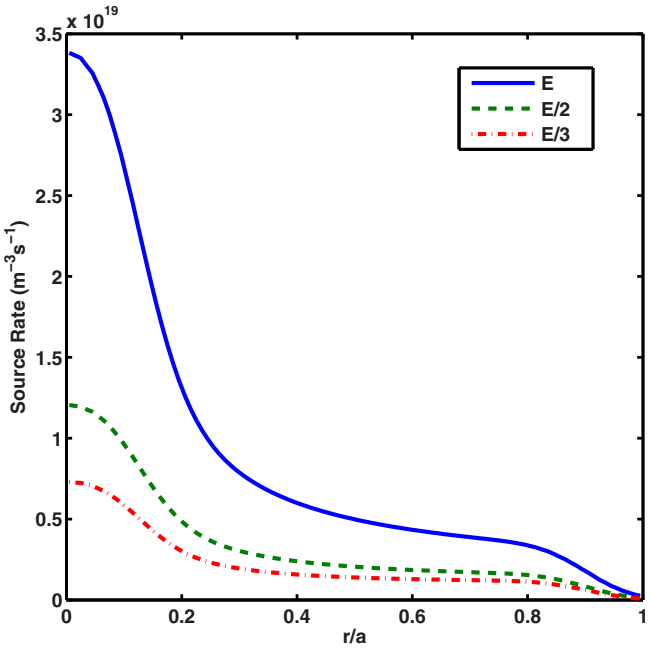

FIG. 2. SOS calculation of NBI source rate profiles for full, half, and third energy component. Details of the case are given in the text.

In the code, for an assessment of the source rate, we reconstruct the flux surfaces assuming an elliptic shape of elongation ε. As representative EAST profiles, we use parametric plasma profiles of the shape, e.g., $n_e = n_e(0)[1-(\frac{r}{a})^2]^\gamma$. Assuming the EAST neutral beam parameters that: P_{beam} = 2 MW, E_{beam} = 80 keV, with $n_e(0) = 3\times10^{19}$ m^{-3}, the calculated source rate profiles for each component are shown in Figure 2, which present the sum of trapped and un-trapped fast particles[8] and are strongly peaked on-axis.

B. D-alpha spectrum predictions

Favorable viewing ports for vertical and tangential geometry, from the vertical B-port and the horizontal O-port, shown in Figure 1, have been decided for FIDA measurements by SOS code, based on EAST plasma data: $n_e(0) = 3\times10^{19}$ m^{-3}, $T_i(0) = 2$ keV, $T_e(0) = 2$ keV, $B = 2.6$ T, $P_{NBI} = 2$ MW, $E(D^0) = 40$ keV/amu, and spectrometer parameters: F-number of 1.8, reciprocal linear dispersion of 1.4 nm/mm, pixel size of 13 μm. Figure 3(a) shows D-alpha spectrum against energy, from the vertical B-port view onto the injected beam at $r/a = 0.1$. In the logarithmic y-axis, it clearly shows that the composite spectrum is consisted of edge lines, MSE part, and FIDA part. The expected FIDA intensity levels are typically 2 to 3 orders of magnitude below the thermal bulk-ion CX feature. The Doppler shift of the MSE is minimised compared to the large spectral width of the slowing-down spectrum. Since the fast ion slowing-down spectrum covers a wide energy range from thermal energies up to the actual beam energy, in this case the high-energy wings of the FIDA spectrum can be separated from the low energy thermal part and compressed MSE spectrum. The clear FIDA signals are expected in the energy range above around 15 keV.

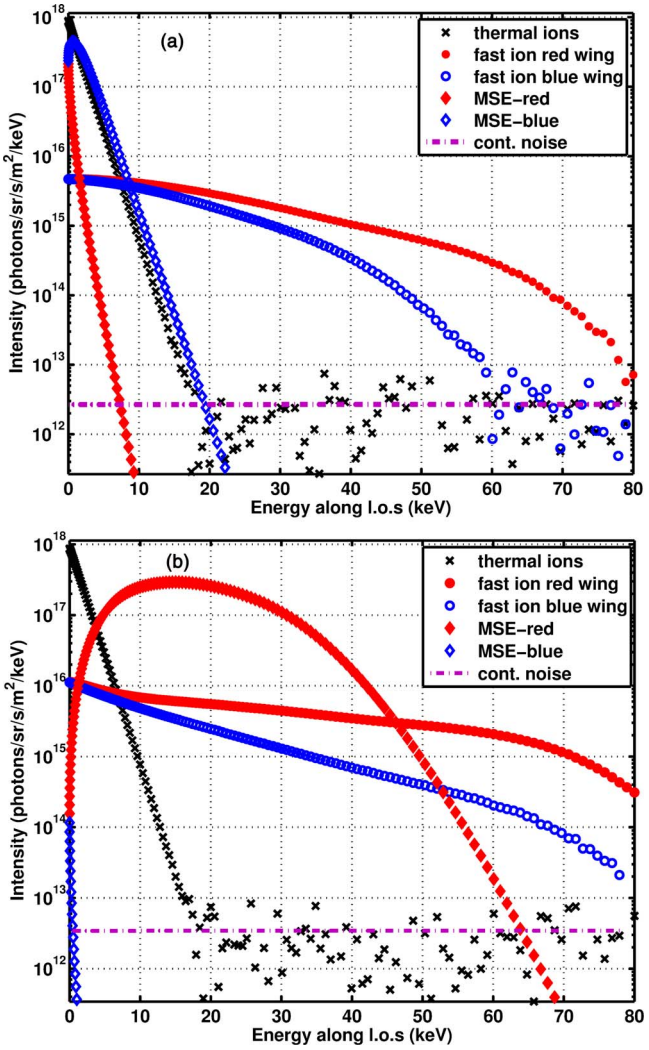

FIG. 3. The calculated D-alpha spectrum at $r/a = 0.1$ against energy, (a) from the vertical B-port view onto the injected beam, and (b) from the horizontal O-port view behind the probe beam together with the future F-port injector. Details of the case are given in the text.

In the case of clear separation of high-energy spectrum from interfering lines, the measurability of the fast-ion feature in the presence of a high continuum background level depends solely on the ratio of the expected FIDA intensities compared to the noise level of the continuum. The continuum noise level determines the signal to noise ratio (SNR),[1] that is the ratio of FIDA signal compared to the fluctuations of bremsstrahlung background plus FIDA signal. Assuming Poisson detector noise characteristics, the SNR depends on the FIDA signal strength Φ_{FIDA}, the continuum noise Φ_{cont}, the detection efficiency $\Re$, and the exposure time $\triangle\tau_{exp}$. With the assumption that the bremsstrahlung counts exceed those of FIDA signal, $N_{cont} \gg N_{FIDA}$, we may therefore write[1]

$$\frac{S}{N} \simeq \frac{N_{FIDA}}{\sqrt{N_{cont}}} = \frac{\Phi_{FIDA}}{\sqrt{\Phi_{cont}}} \cdot \sqrt{\Re \triangle \tau_{exposure}}, \qquad (6)$$

where $\Re$ is $t\eta\varepsilon$ defining the number of counts per radiance,[1] with optical transmission t, quantum efficiency η, and the spectrometer etendue ε. The corresponding SNR is approximately 700, making FIDA measurement feasible.

For the tangential view, in the case of a co- and counter-injection case, fast ion feature will be blue-shifted and red-shifted. The overlaying MSE spectrum will only be present for the probe beam itself. Figure 3(b) shows the D-alpha spectrum against energy, from the tangential view of horizontal O-port along the probe beam at $r/a = 0.1$, together with the future F-port injector. It shows that fast ion feature can only be extracted from the blue wing side, while MSE spectrum dominates the red wing only.

IV. PLANNED LAYOUT AND INSTRUMENT PERFORMANCE

To study the trapped and passing ion features, light are collected from the tangential and vertical views, corresponding to the O horizontal and B vertical port, respectively, as shown in Figure 1. Beam modulation method will be applied for background subtraction to get net FIDA signal. For the vertical view, the paired passive view is also available from the N vertical port shown in Figure 1, allowing direct background subtraction. For the tangential/vertical view, they cover the region from major radii 177–237 cm/177–205 cm, corresponding to 16/8 radial spots with each size at the midplane around 3 cm. Patch panels for the optical fiber with 1500 μm core diameter link from observation ports to the instruments, allowing a flexible combination of ports and instruments. To obtain good spectral resolution and high temporal resolution, respectively, high resolution spectrometers (Kaiser HoloSpec transmission grating spectrometer and Bunkoukeik FLP-200 VPH spectrometer, with F-number of 1.8 and 2, the focal length of 85 mm and 200 mm, the reciprocal linear dispersion of 1.4 nm/mm and 1.28 nm/mm, coupled with Princeton Instruments ProEM 1024B eXcelon and Andor DU-888 iXon3 1024 CCD camera, respectively) and fast filter-based photomultiplier (Hamamatsu model H8711-20) systems will be both available for the complementary measurements.

ACKNOWLEDGMENTS

We would like to express our gratitude to K. Ida for the helpful discussion and J. Li, J. Shen, S. Xia, M. Qi, and F. Fang for the mechanical design and assistance. This is supported by National Magnetic Confinement Fusion Science Program of China under Contract No. 2012GB101001.

[1] M. G. von Hellermann, W. G. F. Core, J. Frieling, L. D. Horton, R. W. T. Konig, and H. P. Summers, Plasma Phys. Controlled Fusion **35**, 799 (1993).
[2] W. W. Heidbrink, K. H. Burrell, Y. Luo, N. A. Pablant, and E. Ruskov, Plasma Phys. Controlled Fusion **46**, 1855 (2004).
[3] M. Podestà, W. W. Heidbrink, R. E. Bell, and R. Feder, Rev. Sci. Instrum. **79**, 10E521 (2008).
[4] E. Delabie, R. J. E. Jaspers, M. G. von Hellermann, S. K. Nielsen, and O. Marchuk, Rev. Sci. Instrum. **79**, 10E522 (2008).
[5] B. Geiger, M. Garcia-Munoz, W. W. Heidbrink, R. M. McDermott, G. Tardini, R. Dux, R. Fischer, V. Igochine, and the ASDEX Upgrade Team, Plasma Phys. Controlled Fusion **53**, 065010 (2011).
[6] M. Osakabe, S. Murakami, M. Yoshinuma, K. Ida, A. Whiteford, M. Goto, D. Kato, T. Kato, K. Nagaoka, T. Tokuzawa, Y. Takeiri, and O. Kaneko, Rev. Sci. Instrum. **79**, 10E519 (2008).
[7] See http://fusionweb.phys.tue.nl/sos for information about the Simulation of Spectra code (SOS).
[8] K.-D. Zastrow, W. G. F. Core, L.-G. Eriksson, M. G. Von Hellermann, A. C. Howman, and R. W. T. König, Nucl. Fusion **38**, 257 (1998).